



**SPE 162034**

## **Electromagnetic sounding in deviated and horizontal wells: mathematical modeling and real data interpretation**

Michael I. Epov, Carina V. Suhorukova, Marina N. Nikitenko, Aleksey A. Gorbatenko, Vitali S. Arzhantsev / Institute of Petroleum Geology and Geophysics SB RAS

Copyright 2012, Society of Petroleum Engineers

This paper was prepared for presentation at the SPE Russian Oil & Gas Exploration & Production Technical Conference and Exhibition held in Moscow, Russia, 16–18 October 2012.

This paper was selected for presentation by an SPE program committee following review of information contained in an abstract submitted by the author(s). Contents of the paper have not been reviewed by the Society of Petroleum Engineers and are subject to correction by the author(s). The material does not necessarily reflect any position of the Society of Petroleum Engineers, its officers, or members. Electronic reproduction, distribution, or storage of any part of this paper without the written consent of the Society of Petroleum Engineers is prohibited. Permission to reproduce in print is restricted to an abstract of not more than 300 words; illustrations may not be copied. The abstract must contain conspicuous acknowledgment of SPE copyright.

### **Abstract**

The features of numerical VEMKZ data interpretation in deviated and horizontal wells entering oil-saturated and water-saturated formations are observed. On the basis of mathematical modeling of VEMKZ signals for typical hole path of horizontal wells the effects caused by crossing bed boundaries and thin layers with high resistivity are shown. The influence of electrical anisotropy on signals has been investigated. The influence of borehole rugosities and tool eccentricity was studied. The programs of numerical modeling have been developed at Institute of Petroleum Geology and Geophysics (IPGG) Siberian Branch of Russian Academy of Sciences.

Algorithms and methodological procedures are used for numerical interpretation of VEMKZ data (including SKL set data) in case of thin reservoir, electrically contrasting shoulder beds and thin interlayers. The eccentricity, borehole rugosity, sine-shaped and spiral well bore influence on signals was investigated in case of typical hole and tool diameters, the programs of numerical correction have been developed. The fact that influence of electrical anisotropy in deviated well causes apparent resistivity increase is demonstrated. Numerical inversion VEMKZ data obtained in well entering terrigenous reservoir underlined by thin layer with high resistivity have been processed. Starting model for inversion is generated by taking direct current data into account. Examples of real VEMKZ data interpretation are demonstrated.

For investigations in deviated and horizontal wells the approach for finding true formation resistivity in thin reservoir using high-frequency induction measurements was proposed. This approach based on numerical signal modeling for deviated tool in horizontally-stratified earth. Algorithms for electrical anisotropy evaluating and thin-layer parameters estimating are observed.

### **Introduction**

Oriented drilling of deviated and horizontal well helps to increase significantly oilfield production effectiveness and so it is extensively used in oilfields. One of the common methods for horizontal well survey in Western Siberia is VEMKZ. Scientific Production Enterprise of Geophysical Equipment 'Looch' (Novosibirsk) produces VEMKZ tool. Widespread wireline version of the apparatus – VIKIZ – is successfully used in additional housing. New set SKL in hard housing provides both BKZ and VEMKZ measurements. SKL set was developed in collaboration of IPGG SB RAS and 'Looch'.

Each VEMKZ probe consists of three coils: one transmitter and two receivers. Each of five transmitters has unique frequency. Each transmitter excepting the most high-frequency coil corresponds to two pairs of measuring coils. Every probe has spacing  $L$  (distance from transmitter to further receiver) and frequency  $f$ . Spacings (m) and frequencies (MHz) of main probes (contained in VIKIZ): 2.0 and 0.875, 1.4 and 1.75, 1.0 and 3.5, 0.7 and 7, 0.5 and 14, additional arrays: 1.6 and 1.75, 1.1 and 3.5, 0.8 and 7, 0.6 and 14. In both main and additional group all the three coil arrays have same parameter  $\sqrt{f}L = \text{const}$ . That provides signal equality for all probes in homogeneous environment. The ratio of spacing between receivers to probe length  $L$  for main group is 0.2, and for additional is 0.18. The most of the devices measure phase shift of voltage at receivers. VEMKZ device in SKL set measures both phase shift and voltage amplitude ratio.

BKZ (Russian lateral logs) tool consist of a number of electrode arrays. Each array includes one current electrode (A) and two receiver electrodes (M and N) which suited upper or lower than current one. Usual BKZ tool consist of arrays with AM length from 0.4 m to 8 m. BKZ-SKL set (Epov et al., 2010) electrodes are suited on tool housing with diameter either 0.076 or 0.102 m, array length from 0.2 m to 4 m.

VEMKZ numerical interpretation method is good developed for vertical wells crossing horizontal geological boundaries. The result of interpretation is radial distribution electrical resistivity. This distribution helps in evaluation of reservoir porosity

and permeability (Kashevarov et al., 2003, Epov et al., 2004). Radial resistivity distribution is a result of mud filtration into porous-permeable layer. It is determined using inversion of VEMKZ and/or BKZ responses. Experience has shown that separate data inversion of these methods can result in not only a set of equivalent resistivity models, but sometimes it results in inconsistent models. Joint inversion in the most occasions helps to overcome this problem. Traditionally there is large time lag between BKZ and VEMKZ measurements. During this time invaded zone may change significantly. The problem of correct coordination this data by depth is also unsolved. Joint inversion VEMKZ and BKZ data measured by SKL tool helps to avoid this problem and to obtain a consistent profile of resistivity.

Numerical interpretation in deviated and horizontal wells is a big problem nowadays. First of all, because such well enter thin reservoirs which have already been worked-out at the most productive parts, and depth becomes deeper and deeper. It is known that as depth increasing the reservoir structure becomes more complicated. Rock solidification and metamorphosis is associated with claying and pyritization. Porosity type in such case changes from intergranular to fractured. Conductive borehole fluid more and more used while drilling. Traditional survey and interpretation methods have been designed for thick homogeneous terrigenous reservoirs decreases, and in these conditions their effectiveness decreases.

As a result, in data from horizontal boreholes we often observe effects caused by lateral inhomogeneities (low-resistive clay lenses, thin limestone, flooded intervals etc.). It is known that iterative thin layers is the reason of resistivity anisotropy which affect responses, especially in case of high angle of well deviation. The influence of a nearby conductive clay layer or oil-water contact reduces apparent resistivity at the interval. The presence of a thin high-resistivity layer may lead to a false conclusion about the oil saturation due to the increase of apparent resistivity.

By that time the programs for numerical modeling VEMKZ responses at deviated and horizontal wells have been constructed. The effect tool eccentricity and the borehole irregularities, filled with conductive fluid have been studied. VEMKZ responses calculated for typical reservoir models have been analyzed. Algorithms for reservoir anisotropy estimation in deviated and horizontal intervals have been developed.

### Borehole and eccentricity effects in wells filled with conductive drilling fluids

During the drilling of deviated and horizontal wells in terrigenous formations are commonly used high conductive borehole fluids with low resistivity (tenths and hundredths of ohm-m). In traditional interpretation methods and algorithms of quantitative inversion it is thought that the tool is on the well axes, but in deviated and horizontal wells the tool is located on the well wall. Also the well doesn't have cylindrical shape. Cavities and fractures filled with high conductive borehole fluid is the case of response distortions. It complicates the visual analysis of these diagrams and can cause incorrect results of interpretation. Thus it is necessary to do preprocessing of this data before the inversion. It can fix influence of the factors, which disturb the obtaining of the reliable resistivity values.

### Borehole irregularity effect

VEMKZ responses measured in wells filled with low-resistivity fluids often have fluctuations with high amplitude and period about 0.5-2.0 m which don't refer to geological formations. These fluctuations may be presented at all the measured interval or at some segments of data. They can be either random or periodic (Fig. 1). Measurements made using another VEMKZ tool give the same result. Moreover, other geophysical methods also can register these fluctuations. It means that this effect is not a special noise but effect occurred as a result of drilling process. In recent years we have collected a lot of such data from various oilfields at Western Siberia.

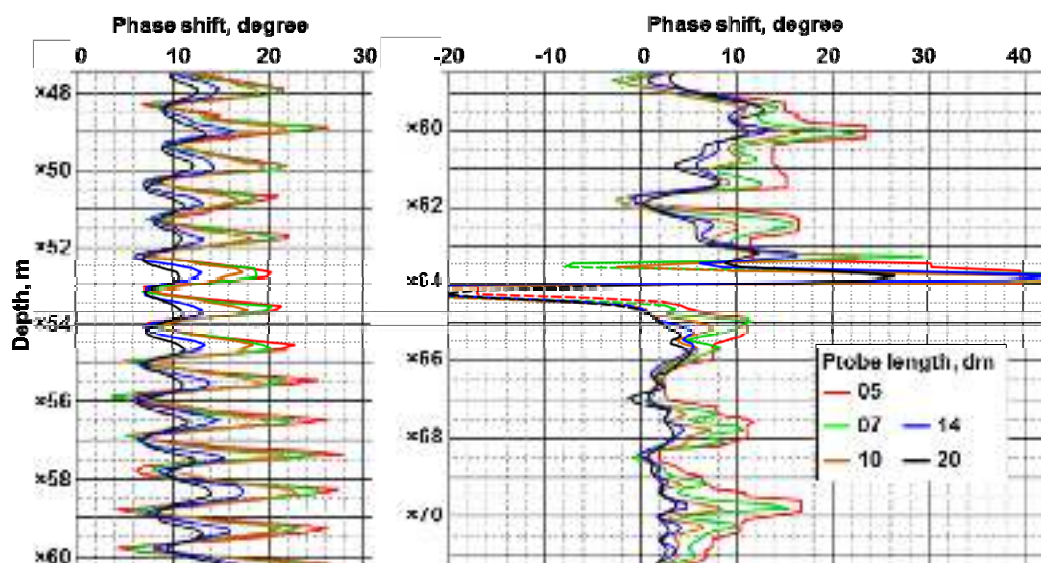


Fig. 1. Real VEMKZ signals.

After analysis of possible models which could cause such effects we made following conclusions. Non-cylindrical borehole shape may result from both vertical (Gubina et al., 1997) and oriented drilling, in particular with rotary steering systems (Zykina, Mamyashev, 2007). In addition to keyseats borehole may have corkscrew shape. Chaotic noises and single spikes correspond to strongly fractured intervals or single deep caverns and fissures.

In this case there are low resistive areas near borehole and their responses affect both phase shift and amplitude ratio. Correlation between caliper and VEMKZ (Fig. 2) data proofs that this response distortion refers to high extent of borehole rugosity. It is also noted that the noises and fluctuations are absent at coring intervals. Periodic fluctuations in the diagrams can also arise deviated well enters interval with interbedding of thin clay and sand layers (Antonov, 2006).

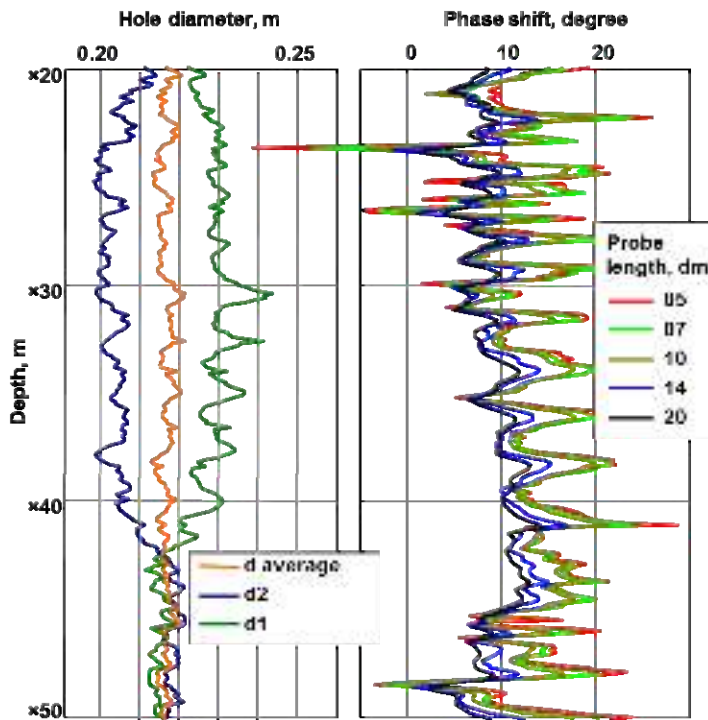


Fig. 2. Caliper (left) and VEMKZ phase shift (right) diagrams. Borehole resistivity 0.09 ohm-m.

Numerical modeling showed that ring-type symmetric cavern first is decreasing and then increasing the phase shift and amplitude ratio while device moves up (Fig. 3). The amplitude of oscillation is proportional to the depth of the cavity.

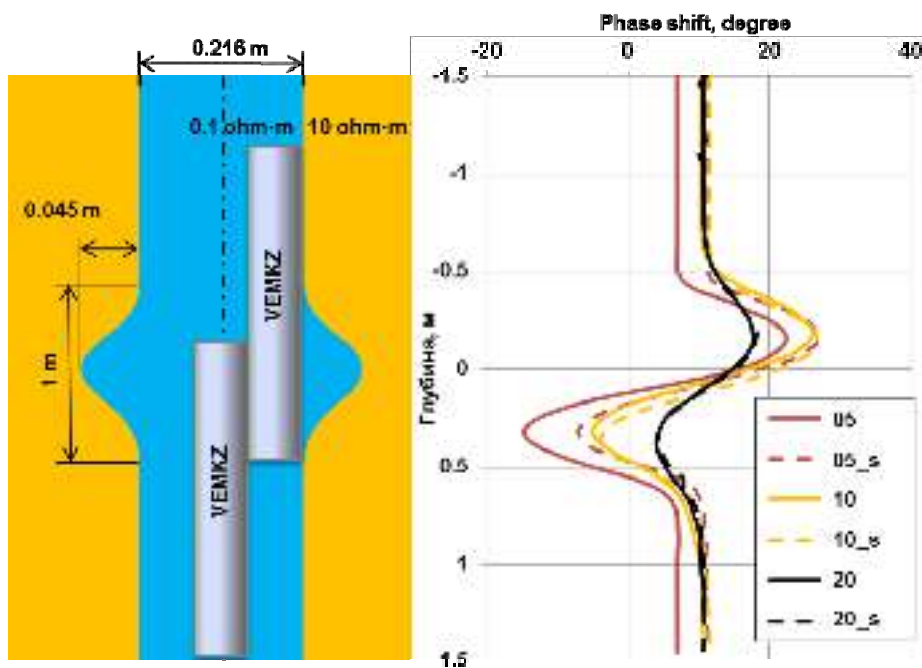


Fig. 3. The model with a single cavity. The phase shift between have been calculated for tool which is located on the axis (solid lines) and wall (dotted line) of the well.

The average signal level and the amplitude of the fluctuation are nonlinearly dependent on the formation resistivity. For all the arrays, the oscillation amplitude for both phase shift and amplitude ratio increase rapidly as formation rises. But oscillation amplitude is almost constant when formation resistivity reaches 10 ohm-m. However, even rugosity which causes high-amplitude oscillation doesn't change average value of diagram in thick homogeneous formations. It means that we can easily reduce the fluctuations using simple filtration algorithms.

The same signals are calculated in the well with a constant cross-sectional diameter, but the sinusoidal or spiral hole track (Fig. 4). In this case fluctuation period is equal to the period of the spiral hole. In case of sine well it is a half of the sinusoid period.

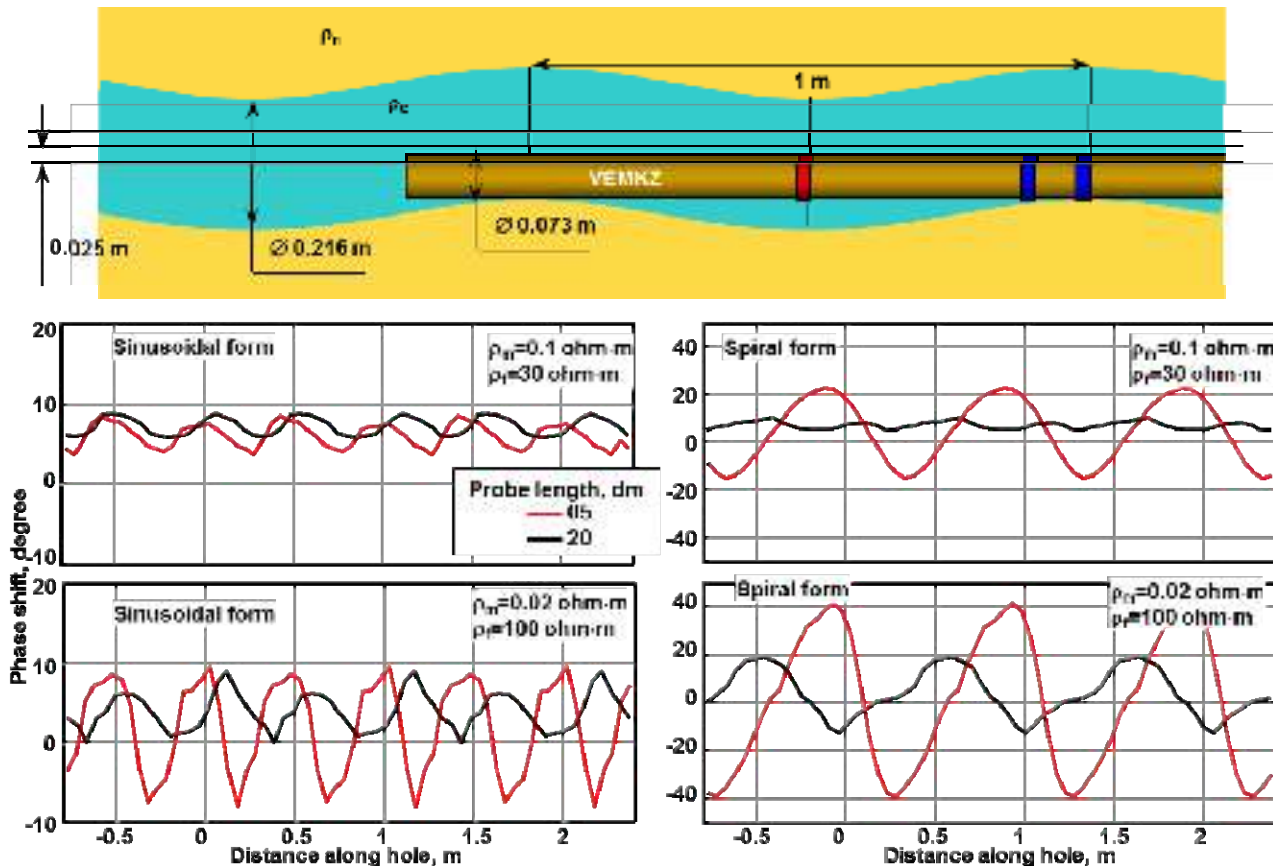


Fig.4. Responses in spiral and sine wells.

#### Influence of tool eccentricity

Typically, the inversion algorithms assume that at the time of measurement, the unit is on the axis of the borehole. But usually wireline logging tool lies on the borehole wall. In this case, electromagnetic field produced by the generator, will cross the well-formation border. As a result, electrical charges will appear and affect responses (Ignatov, Sukhorukov, 2009). This can result in either increase or decrease (depending on the situation) of the phase shift and amplitude ratio. Therefore, corrections suppressing standoff effect should be made before numerical VEMKZ data interpretation.

Difference between responses at the wall and at the axis is presented at Fig. 5. (typical diameter of a horizontal well 0.124 m, VEMKZ housing diameter 0.102 m). Tool standoff strongly affects the shallowest sonde, but for sondes longer than 1 m the effect less than measurement error. And this tool decentralization changes the phase shift is greater than the amplitude ratio. Note that when the mud resistivity is low tool standoff increases the phase shift and decreases the amplitude ratio.

The developed algorithm allows to exclude the influence of standoff, using master charts, which calculated by means of vector finite element method. In these charts the model takes into account non-conductive tool housing, borehole resistivity ( $R_m$ ), formation resistivity ( $R_t$ ) and actual diameter of transmitter and receiving coils (Epov et al, 2007). The algorithm allows construct transformation from the measured signal in the apparent resistivity considering borehole and standoff as well as recalculate responses axial sonde position for following interpretation.

The bigger well diameter and shorter sonde the higher standoff influence. Fig. 6 illustrates application of standoff effect correction algorithm for real data from wellbore with big diameter (0.216 m), and mud resistivity (0.16 ohm-m). At the diagrams of measured responses sandstones (gamma ray value about 5-7 mkR/h) differ only a little from clay (8-10 mR/h) by discrepancy between apparent resistivity of different VEMKZ coil arrays. After the correction apparent resistivity values of different sondes become almost equal at clay intervals and noticeable discrepancy noticeable discrepancy is only in the perme-



able sandstone intervals ( $\times 85 - \times 121$  m, excepting of clay and limestone layers). Comparison charts before and after taking into account the eccentricity shows a strong change in the values  $R_a$  for the shallowest sonde (3-7 ohm·m), whereas the values for the deepest sonde are almost the same.

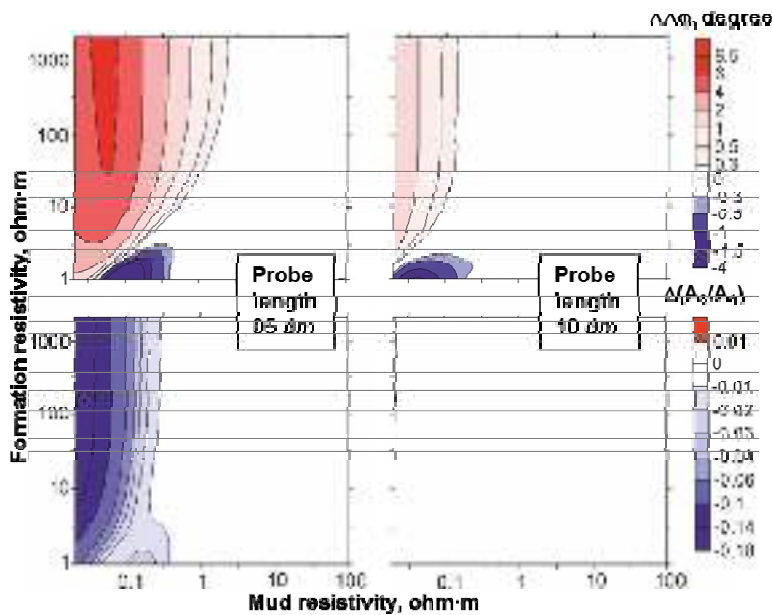


Fig. 5. Difference between signals of the tool at the axes of the well and at the wall.

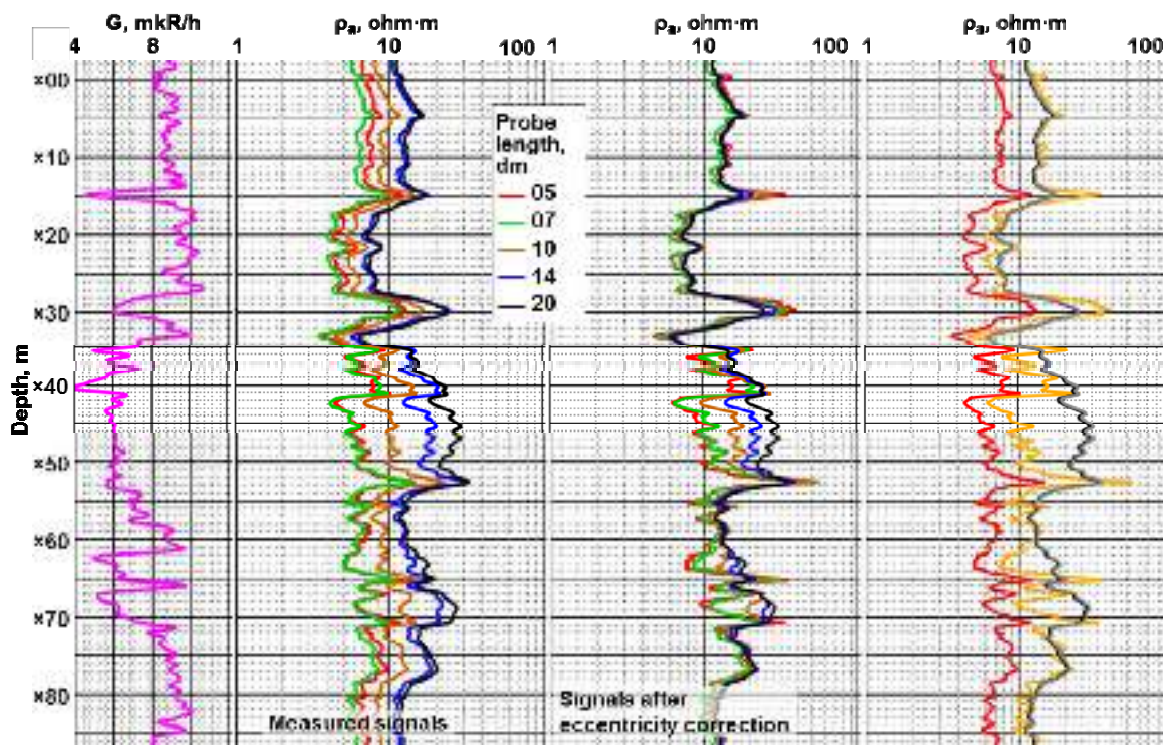


Fig. 6. Eccentricity correction. Charts: left – gamma ray, next – VEMKZ apparent resistivity, measured and corrected to the axis. The right chart – comparison of measured and corrected signals for short probe (red and orange lines) and long probe (gray and black lines).

Thus, shallow hole rugosities resulted from drilling process cause single or periodic fluctuations on VEMKZ logs. But the average signal level corresponds to the signal in a smooth hole. Therefore, before visual or numerical interpretation filtering of signals is reasonable. In a large range of mud resistivity and formation resistivity effect of eccentricity on the signal long coil arrays does not exceed the measurement error, so the inversion of the data in this case can be used without correction. If formation/borehole resistivity contrast is high the eccentricity results in artifacts in form of false penetration zones. But if we took

into account influence eccentricity form of penetration is not distorted. The algorithms of efficient numerical correction for the influence of the borehole wall roughness and tool eccentricity have been constructed.

### Numerical modeling of VEMKZ signals

For the numerical modeling of VEMKZ data in deviated wells drilled through horizontally layered anisotropic medium the algorithms and software have been developed and produced in IPGG SB RAS.

One of the algorithms based on solving the problem of a harmonic electromagnetic field of magnetic dipoles excitation in a horizontally layered earth, each layer is described by resistivity, which is equal in horizontal and vertical directions. The program provides a quick calculation of the signals for the thousands of positions of the transmitter and receiver in medium consisting of hundreds of layers. This enables the use of the algorithm for solving the inverse problem. However, borehole environment and invaded zone are not considered. At the previous section we showed that near-field zone almost doesn't have influence to deep reading measurements. Therefore, long-spaced arrays and a horizontally layered medium should be used for the automatic inversion.

Algorithms using the models with borehole and invaded zone based on the finite-difference schemes and vector finite element method (Epov et al, 1999, 2007, Surodina, 2012). Their software implementations are very resource-intensive. Thus, it is impossible to solve inverse problem using these algorithms, although in our experience there are a few examples of the "inversion" with manual enumeration of model parameters. Calculations of the signals for the most realistic mediums, tool and well are mainly used for the analysis of typical geoelectrical situations. The calculation results can justify techniques of numerical signal processing.

### Typical models and tack of wells with horizontal completion

Consider typical model for the upper part of oil-bearing reservoir, overlaid by clay deposits (Fig. 7). The calculation has been made for horizontal beds. Clay resistivity is 4 ohm·m, resistivity of reservoir is 15 ohm·m. Well track (at the top of Fig.7) is typical for conditions of Western Siberia. Apparent resistivity has been calculated using phase shift ( $\rho_a(\Delta\phi)$ ), at the middle) and amplitude ratio ( $\rho_a(A_2 / A_1)$ ), downward) for 9 sondes.

It is known that when VEMKZ tool passes bed boundary electrical charges proportional to formation resistivity contrast ratio will appear at this boundary. These charges affect the signals. This influence is particularly strong for phase shift ( $\Delta\phi$ ): there are local maximums at the phase shift charts which are corresponded to border crossing points. The more well inclination the higher the spikes. Response from the second layer appears at the intervals where distance from border to receivers less than offset from transmitter to nearest receiver ( $L_1=0.8L$ ), at the reservoir apparent resistivity decreases to 13 ohm·m and at clay it increases to 6-7 ohm·m. All the apparent resistivity values reach true reservoir resistivity only in the lowest part of well (80-200 m), these point are located further than for the deepest sonde ( $L_1=1.6$  m) from border. At the more conductive clay charge response a bit lower and apparent resistivity reaches clay resistivity at a smaller distance from the border – about 0.6  $L$ . True clay resistivity showed by sondes with length 0.5-1.1 m. At the interval where the well goes almost along the border VEMKZ curves are diverging and using traditional interpretation techniques for vertical wells we would conclude that there is an invaded zone with resistivity ( $R_{xo}$ ) >  $R_t$ . The fact that curves of main and additional are also diverging could be used to distinguish effects of border influence and radial inhomogeneity of reservoir resistivity.

Amplitude ratio ( $A_2 / A_1$ ) is less influenced by the charge than phase shift. There is no big maximums at the charts and border crossing is fixed by low-amplitude spikes. The  $A_2 / A_1$  curves of two the deepest sondes don't reach value of reservoir resistivity. Sondes with lengths from 0.5 to 0.8 reach value of clay resistivity. The fact that for  $A_2 / A_1$  shoulder effect is more significant than for  $\Delta\phi$  appears because for amplitude ratio field of investigation is bigger than one for phase shift (Glinskikh, Epov, 2005). At the interval of the well near the border the curva are also divided into two groups: main and additional. But difference between curve values into one group is quite small.

For the water-saturated reservoirs in Western Siberia resistivity values are the same as for clays. Therefore, the following model is a reservoir divided into oil-water-saturated and water-saturated parts with resistivity of 15 ohm·m and 4 ohm·m.

The lowest point is in the water-saturated part the depth of 0.8 m (Fig. 8). When tool is crossing the border, as in the previous case, there is a sharp increase of  $R_a(A_1/A_2)$ . The influence of the more conductive lowest part affects at the same distance to the border (less than 0.8  $L$ ) in the same lowering of values. In the water-saturated part values of  $R_a(\Delta\phi)$  curves reach the formation resistivity for sondes from 0.5 to 1.6 m in length, for  $R_a(A_1/A_2)$  true resistivity is reached by sondes 0.5 – 0.7 m. In the horizontal interval of the well at the distance 2 m from the border all the  $R_a(\Delta\phi)$  values are equal to resistivity of the oil-water-saturated part, but  $\rho_a(A_2 / A_1)$  for 1.1-2.0 m probes are affected to influence of the lowest part, which decrease their resistivity to 13 ohm·m.

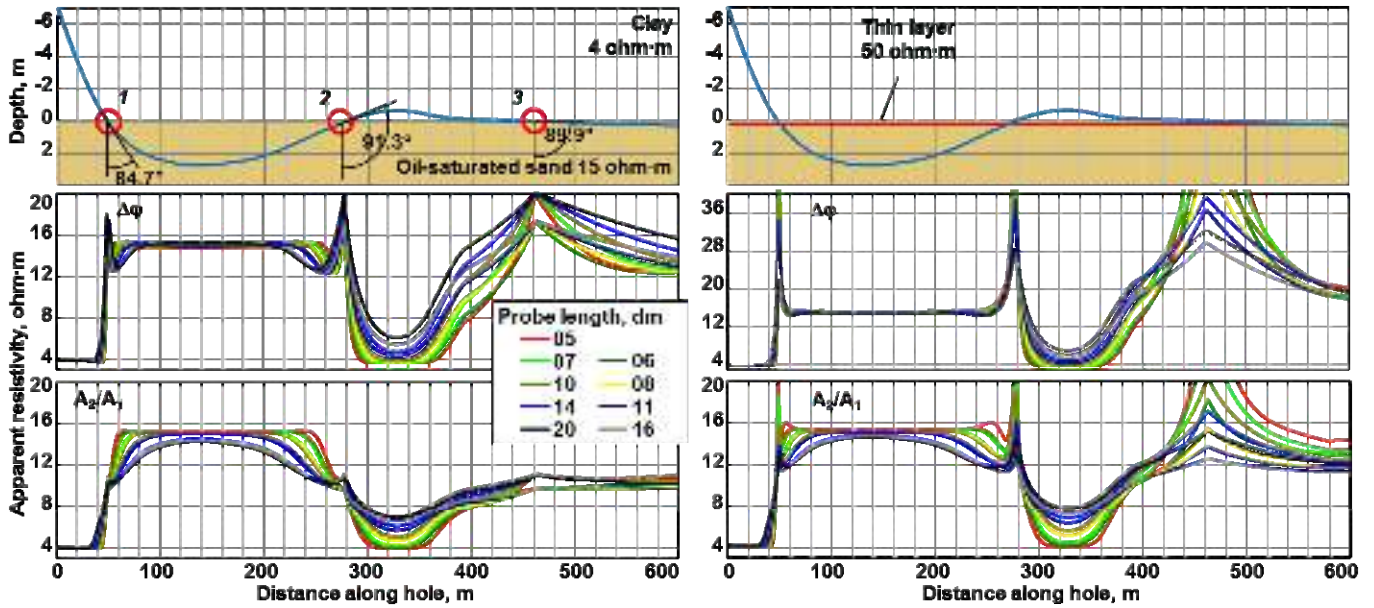


Fig. 7. The model of well with horizontal completion, crossing reservoir and apparent resistivity charts. Red cycles mark points where border crossed. At the right – the same model but with high-resistive interlayer at the roof of reservoir.

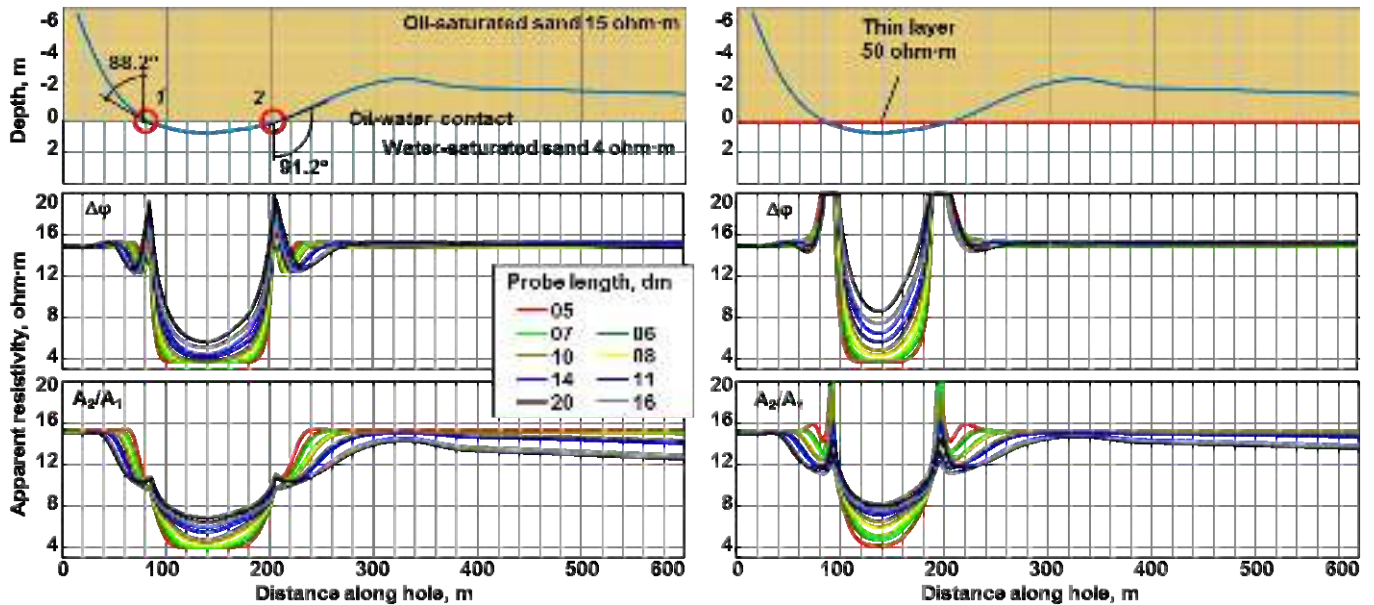


Fig. 8. The model of well with horizontal completion, crossing oil-water contact and apparent resistivity charts. Red cycles mark points where border crossed. At the right – the same model but with high-resistive interlayer at the contact.

At a higher position of the well (Fig. 9) the influence of the more conductive lower part occurs in points located at a distance less than  $L$  for  $\rho_a(A_2/A_1)$  and less than  $1.5L$  for  $\rho_a(\Delta\phi)$ . In the interval, where the well is closer than  $0.5L$  to the border, apparent resistivity at the  $\rho_a(\Delta\phi)$  chart increases and reaches maximal value at the lowest point of the well (0.3 m from border).

If we add to the model thin resistive layer (usually it is carbonated sandstone with resistivity 30-100 ohm-m) it would significantly change  $\rho_a$  near the border. In following examples the layer with thickness 0.2 m and resistivity 50 ohm-m placed at the border (Fig. 7-9, right). In the model at the Fig. 7 maximum values  $\rho_a(\Delta\phi)$  near the border highly increased and under the border was almost imperceptible lowering effect of clay,  $\rho_a(\Delta\phi)$  in the sub horizontal interval are significantly enhanced. At the  $\rho_a(A_2/A_1)$  chart maximums appeared where well crosses the boundary. In the model at the Fig. 8 near the border maximum values of  $\rho_a(\Delta\phi)$  also increased and  $\rho_a(A_2/A_1)$  maximums appeared, under the border lowest number of curves reached true formation resistivity of the lowest part. In the subhorizontal part of well conductive part of reservoir influence low-frequency long sondes only. At the Fig. 9 influence of the lowest medium to phase shift becomes even smaller. At the



lowest part of the well high resistive layer increased  $\rho_a$  for both parameters and changed form of shallow  $\rho_a (A_2 / A_1)$  curve.

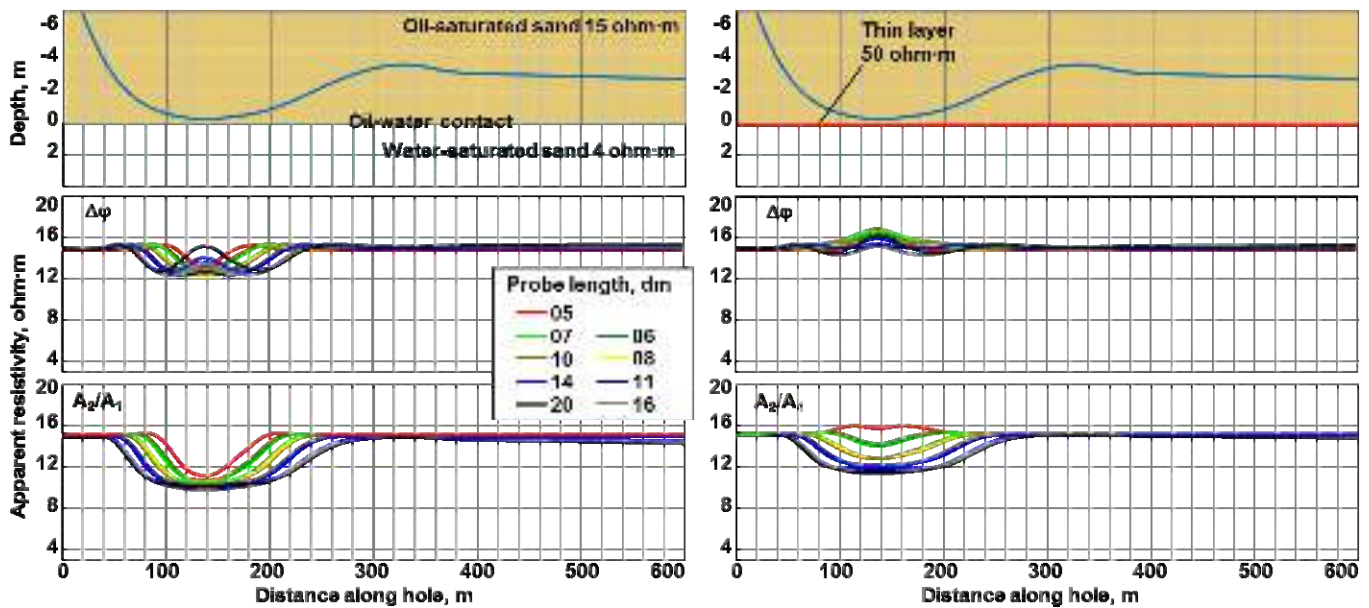


Fig. 9. The model of well with horizontal completion near oil-water contact and apparent resistivity charts. At the right – the same model but with high-resistive interlayer at the contact.

In general, increasing the resistivity of high-resistance interlayer leads to raised resistivity contrast and even greater spikes when tool crosses borders and less dependence on the medium located on the other side of interlayer. Note that the interlayer with these parameters is not reflected in the signals of induction logging in vertical wells.

The calculations show that in deviated and horizontal wells VEMKZ signals don't depend on surrounding rocks and contrasting interlayers in beds twice thicker than sonde length. At the middle of this layer  $\rho_a (\Delta\phi)$  and  $\rho_a (A_2 / A_1)$  will be equal to true formation resistivity excepting the deepest curves. However, characteristic behavior of the signals near the boundaries and singlevalued dependence on contrast of electrical properties allows to find formation parameters using the program for modeling responses of deviated tool in case that well track is known.

Calculation of the signal in the realistic model (including borehole) shows that the main features curve features are stored; the only change is the extremes caused by charges at the boundaries - sharp spikes characteristic for short sondes smooth out (Fig. 10). The signals of long sondes (Epov, Martakov et al, 1999) are practically independent on the conductive solution in the borehole. In practice, commonly used diameter of the hole is 0.124 m, so the impact is even less.

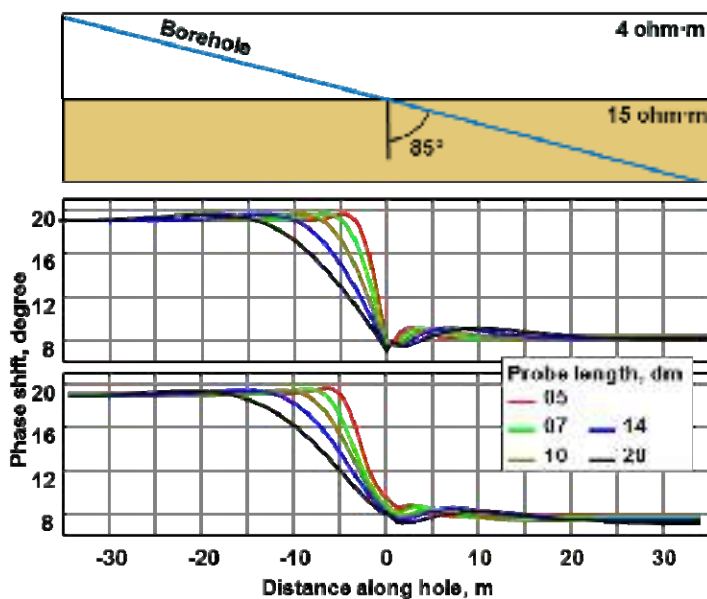


Fig. 10 Comparison of signals calculated without borehole (at the center) and with it.



### Electrical macroanisotropy

Complex measurement system is assumed to be necessary for formation electrical anisotropy evaluation. Many companies construct induction devices with both coaxial and perpendicular moments of transmitter and receiver coils, all the sondes employ many frequencies. However, simple system of coaxial to well coil arrays employed in both low-frequency and high-frequency systems are also dependent on vertical resistivity (Epov, Suhorukov et al, 1999). High frequencies of VEMKZ provide possibility of anisotropy evaluation in deviated wells crossing transversely isotropic formations. To estimate parameters of anisotropy information given a priori is used, for example, resistivity measured in horizontal well and geological data.

Electrical macroanisotropy complicates reliable investigation of thin-layered reservoirs crossed by deviated or horizontal well. In general, the plane of the thin interbedding may lie unconformably to the borders of the reservoir. As follows from geological data and preliminary evaluation, angle between borders and direction of interlaying varies within wide limits (up to  $30^\circ$ ).

Thus, to describe thin-layered reservoirs crossed by deviated well it isn't enough to use only one parameter. In this case it is advisable to use three: horizontal apparent resistivity  $\rho_a^h$ , vertical apparent resistivity  $\rho_a^v$  and inclination angle  $\theta_a$ . In isotropic medium  $\rho_a^h = \rho_a^v = \rho_a$ . In this situation we cannot define angle  $\theta_a$ , we only can use directional survey data  $\theta_a = \theta$ . To find all three parameters we need an least three measurements. Since every measurement has errors the number of measurements have to be bigger than number of parameters to get reliable result. Homogeneous transversal isotropic medium have been chosen as interpretation model. Its resistivity is described by  $\rho_v$  and  $\rho_h$  parameters (resistivity perpendicular to bedding plane and parallel to it). We assume that the horizontal plane coincides with the strata (Fig. 11).

Dependence of phase shift on angle between tool and the plane of stratification is the same for all the sondes (Fig. 11, right). In vertical well apparent resistivity and phase shift correspond to isotropic resistivity, which is equal to  $\rho_h$ . In horizontal well they are equal to  $5.4^\circ$  and 28 ohm·m. In horizontal well  $\rho_a$  is 0.7-0.8 of  $\rho_v$ . For example, at the reference interval of clay in Western Siberia  $\rho_a$  in vertical well is 4.4 ohm·m, in highly deviated wells - about 8 ohm·m. Therefore  $\rho_v$  is about 10-11 ohm·m

Consider VEMKZ signal in anisotropic formation. At Fig. 12 phase shift is illustrated. Since  $\rho_v$  cannot be less than  $\rho_h$ , the part of the picture upper then bisecting line  $\rho_v = \rho_h$  corresponds to isotropic media with resistivity equal to  $\rho_h$ . Pay attention to changes in the phase shift in an anisotropic medium with an increase in the angle between the tool and the plane of strata.

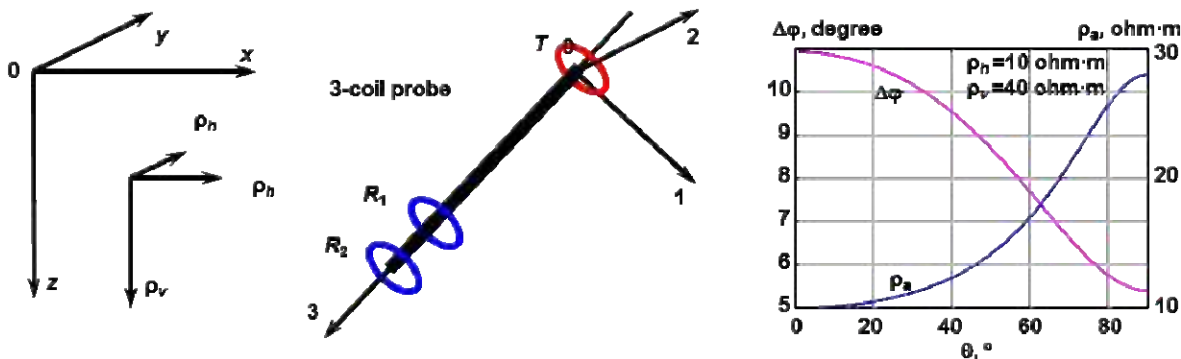


Fig. 11. Main and additional coordinate systems and dependence of phase shift and apparent resistivity on angle  $\theta$  in homogeneous medium (left).

For angle  $\theta = 40^\circ$  isolines of  $\Delta\phi$  are almost horizontal. Anisotropy is of small influence to the responses. We can obtain the same value of  $\Delta\phi$  changing  $R_v$  at the almost whole range. Consequently, at small angles  $\theta$  we cannot establish  $R_v$  by the phase shift value.

For angle  $\theta = 60^\circ$  phase shift dependence on  $R_v$  becomes big enough to find only one value  $R_v$  for one  $R_h$  at  $\Delta\phi$  isolines. Such slope at the plots is typical for  $R_v/R_h$  less than 2. At the same time  $R_h$  range is quite small. For example, for isoline  $\Delta\phi = 10^\circ$  horizontal resistivity is between 3.2 and 11.4 ohm·m with  $R_v$  range from 11.4 to 100 ohm·m. It may result in significant errors in  $R_v$  estimation using measurements of small phase shift with measurement error.

With further increase of the angle  $\theta$  form of isolines varies greatly. With  $\theta = 80^\circ$  isolines corresponded to low values of phase shift going down to  $R_v = R_h$  approach some maximum value of  $R_v$ . After that little decrease of  $R_h$  corresponds to significant decrease of  $R_v$ . For example, isoline  $\Delta\phi = 5^\circ$  begins with values  $R_v = R_h = 31.2$  ohm·m, then it almost straightly goes down to  $R_h = 12.2$  and  $R_v = 50.7$  ohm·m, and after changing of direction it goes to point  $R_h = 2.0$  and  $R_v = 15.9$  ohm·m. There is field of negative phase shift with very low values of  $R_h$  (less than 2 ohm·m) and high values of  $R_v$  (more than 42 ohm·m).

These patterns are stored for values of  $\theta$  up to  $90^\circ$ . Isolines almost don't depend on  $\theta$  from  $85^\circ$  to  $90^\circ$ . Compared with  $\theta = 80^\circ$ , in the case of horizontal tool position points with a maximum of  $R_v$  shifted towards higher values of  $R_h$  and smaller  $R_v$ .

For the isoline  $\Delta\varphi = 5^\circ$  this point moves from coordinates indicated above to the values  $\rho_h = 13.5$  and  $\rho_v = 46.5$  ohm·m, Minimum of  $\rho_v$  also decreases (up to 13.2 ohm·m for the same isoline).

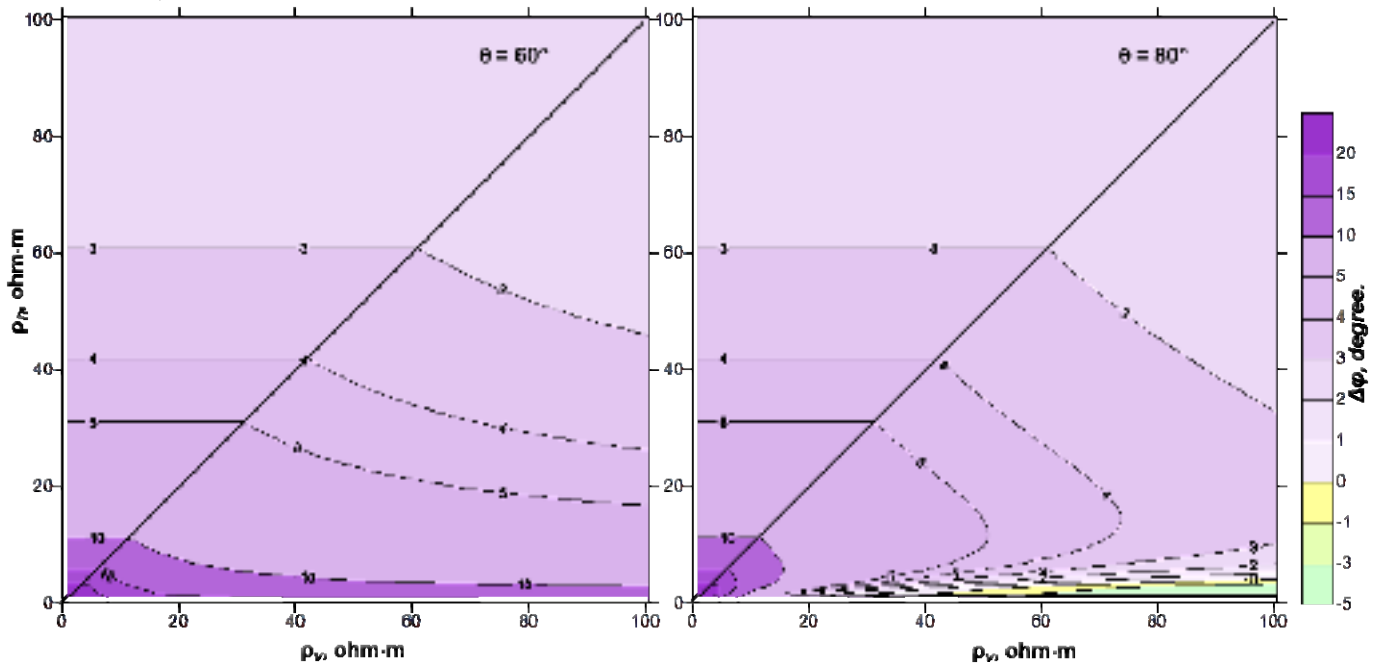


Fig. 12. Isolines of phase shift in anisotropic medium:  $\theta = 60^\circ$  (left) and  $80^\circ$  (right).

## Inverse problems

### Low-thickness reservoir

Let's execute inversion of signals of two long VEMKZ probes in model with crossing of a top of a reservoir with a high-resistance pro-layer (Fig. 7, on the right). As already noted, long probes get out because their signals aren't influenced practically by a well, a invaded zone and eccentricity. The program of automatic inversion is based on algorithm of minimization by a Nelder-Mead method of relative least-square residual function for synthetic and experimental signals:

$$F^{nz} = \frac{1}{N_p - 1} \sqrt{\sum_{i=1}^{N_p} \left[ \frac{\Delta\varphi_i^{nz} - \overline{\Delta\varphi_i^{nz}}}{\delta\Delta\varphi_i^{nz} \cdot \Delta\varphi_i^{nz}} \right]^2}.$$

Here  $N_p$  is number of registration points on depth,  $\Delta\varphi_i$  is the measured phase shift,  $\delta\Delta\varphi_i$  is an error of measurement,  $\overline{\Delta\varphi_i}$  is the phase shift calculated in a layered homogeneous environment,  $nz$  is a probe index. Residual function is calculated for each probe.

The number of points on a well is equal 600, the hole inclination is set in each point according to inclinometer. Horizontal border location ( $z_1, z_2$ ) and layers resistivity ( $\rho_1, \rho_2, \rho_3$ ) are varied parameters. Starting value on the first iteration gets out taking into account possible errors of parameter estimation. The result of work of the program is given in the table.

Table. Results of automatic inversion.

Model parameter	$\rho_1$ , ohm·m	$\rho_2$ , ohm·m	$\rho_3$ , ohm·m	$z_1$ , m	$z_2$ , m
<b>1st iteration</b>					
Starting value	4.5	40.0	17.0	0.10	0.40
Inversion result, 105 steps	4.1	33.2	14.9	-0.005	0.34
<b>2nd iteration</b>					
Inversion result, 62 steps	was fixed	52.0	was fixed	0.0002	0.19
<b>3rd iteration</b>					
Inversion result, 76 steps	4.1	47.4	15.0	0.0002	0.21
True value	4.0	50.0	15.0	0.00	0.20

Resistivity of a clay cap rock and reservoir is reconstructed at the first iteration with sufficient accuracy for practice. Paires of parameters of a high-resistance interlayer (resistivity and thickness), equivalent on longitudinal conductivity (thickness/resistivity), are specified at the subsequent iterations.

Let's consider an example of practical data inversion. Fig. 13 shows result of geoelectric model reconstruction on way-down well interval. Depth of registration points on a well, the location of the main borders and the vertical resistivity distribution are shown in an average part of figure. Comparison of phase shift values measured by a long probe and calculated in reconstructed model, is shown at the figure top. At inversion the angle between borders and the horizontal plane was determined also. The specified value is equal  $1.2^\circ$ .

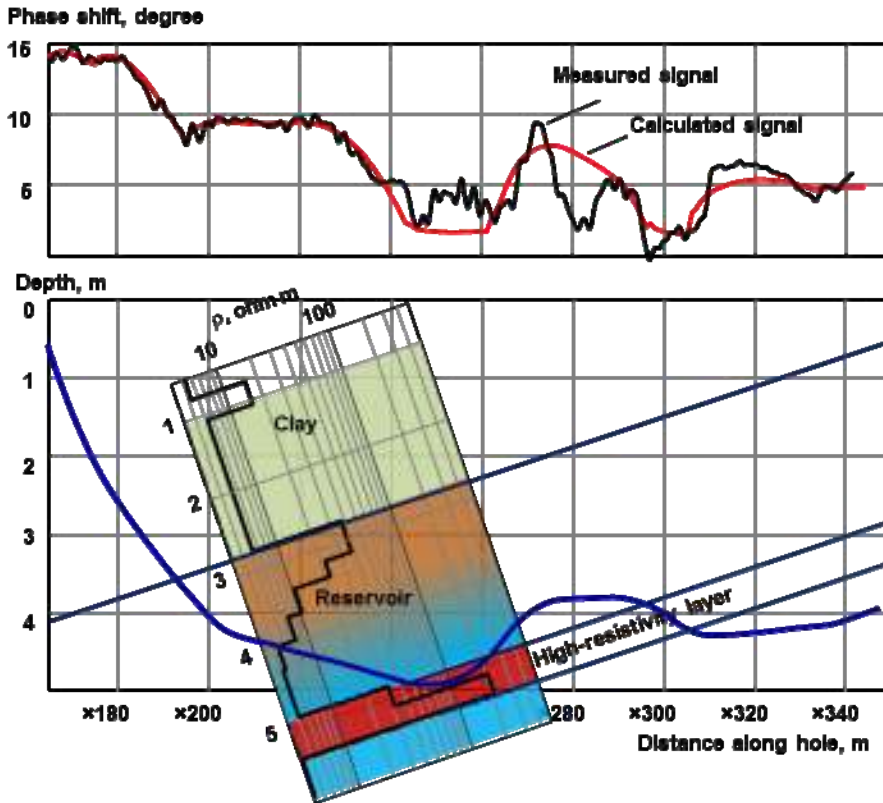


Fig. 13. Measured and calculated phase shift values (long probe, at the top), relative depth of well points and the inversion resulting model (vertical resistivity distribution).

Resistivity decreases from a top to a bottom with 36 to 5 ohm·m that corresponds to normal vertical distribution in oil and water saturated reservoir. The high-resistivity non-permeable layer underlying a reservoir, is crossed by a well on intervals of  $\times 245\text{--}\times 260$  and  $\times 295\text{--}\times 310$  m. Probably, on the first interval the layer is partially destroyed when drilling therefore the measured signal shows smaller resistivity, than synthetic. Lower part of a reservoir contains lateral heterogeneity (on an interval of  $\times 260\text{--}\times 295$  m) which parameters can't be estimated as their borders aren't subhorizontal.

### Anisotropic formation

Determination of  $\rho_h, \rho_v$  and dip angle values also can be formulated as a inverse problem. To minimize influence on signals of a near-hole zone inhomogeneity, we will choose responses of the longest probe for inversion  $\{\Delta\varphi_{5,i}, i = 1, \dots, N_p\}$ . It is possible to write down

$$\overline{\Delta\varphi}_{5,i} = \Phi(\rho_h, \rho_v, \theta)$$

Here  $\Phi$  is the direct problem operator,  $\overline{\Delta\varphi}_{5,i}$  are synthetic signals in homogeneous anisotropic environment,  $\theta$  is an angle between borders and a well. Relative errors of measurement we will designate  $\{\delta\Delta\varphi_{5,i}, i = 1, \dots, N_p\}$ .

Let's make a functional corresponding to the relative least-square residual function for synthetic and experimental signals

$$F = \frac{1}{N_p - 1} \sqrt{\sum_{i=1}^{N_p} \left[ \frac{\Delta\varphi_{5,i} - \overline{\Delta\varphi_{5,i}}}{\delta\Delta\varphi_{5,i} \cdot \Delta\varphi_{5,i}} \right]^2}$$

If value of a functional  $F \leq 1$ , an average relative deviation of synthetic signals from the experimental don't exceed relative errors of measurement. Therefore, it is possible to define apparent parameters  $\rho_a^h, \rho_a^v, \theta_a$ , having solved the following nonlinear inequality

$$\frac{1}{N_p - 1} \sqrt{\sum_{i=1}^{N_p} \left[ \frac{\Delta\varphi_{5,i} - f(\rho_a^h, \rho_a^v, \theta_a)}{\delta\Delta\varphi_{5,i} \cdot \Delta\varphi_{5,i}} \right]^2} = \min < 1.$$

All three of the values  $\rho_a^h, \rho_a^v, \theta_a$ , satisfying to this inequality, are apparent values. It is clear, that such three there can be not one. In this case there is a choice problem from a set of equivalent results. Their number can be essentially reduced by introduction of additional restrictions. The first restriction consists in that the maximum discrepancy between synthetic and experimental data didn't exceed the maximum relative error of measurement

$$\max_{i=1, \dots, N_p} \left[ \frac{\Delta\varphi_{5,i} - f(\rho_a^h, \rho_a^v, \theta_a)}{\Delta\varphi_{5,i}} \right] \leq \max_{i=1, \dots, N_p} \delta\Delta\varphi_{5,i}$$

The angle choice between a well and the layer border, the closest to value on an inclinometer can be the second additional criterion

$$|\theta_{a,i} - \bar{\theta}_i| = \min_{i=1, \dots, N_p}$$

Here  $\bar{\theta}_i$  is average value of an angle value measured by inclinometer.

It is known that not less than three measured values are necessary for determination of three unknown parameters. If to consider that measurements are executed with some error, obtaining the stable solution needs their bigger number. It is most appropriate to apply algorithm such as "a sliding window". For this purpose the window of a certain width of  $N_w$  gets out.  $N_w$  is odd number of points which considerably exceeds number of defined parameters ( $N_w \gg 3$ ). In this window the inverse problem is solved, and  $\rho_a^h, \rho_a^v, \theta_a$  values which referring to the window middle are defined. After that there is a window shift on two points and procedure of parameters evaluation repeats. After passing on all interval sets of parameters values will be received

$$\{\rho_{a,i}^h, \rho_{a,i}^v, \theta_{a,i}\}, i = N_w/2, \dots, N_p - N_w/2.$$

Thus, number of points in which parameters are defined, is less total number of points on  $N_w$ . For example, at width of a window  $N_w = 10$  and a digitization step  $\Delta z = 0.2$  m reduction of length of an interval will make 2 m.

The success of the inverse problem solution in many respects depends on a right choice of initial values of determined parameters. For an angle  $\theta$ , such initial approach is its value measured by inclinometer. Initial values of horizontal and vertical resistivity in the first window can be put equal to apparent resistivity in homogeneous isotropic medium:  $\rho_a^h = \rho_a^v = \rho_a$ .

In each following window as initial values results of inversion in the previous window are used.

#### **Inverse problem on the basis of use of equivalence areas**

Let's consider a situation when one of the most real additional restrictions given earlier is carried out:  $|\theta_{a,i} - \bar{\theta}_i| = \min_{i=1, \dots, N_p}$ .

This condition is observed in layers where thin interlayers lie according to their borders. Such statement is allowed in most cases. In this case it is not required definitions of a corner of a meeting of a probe with thin pro-layers. The corner gets out of inclinometriya data. Then it is not required definitions of angle of a meeting of a probe with borders. The angle gets out of inclinometer data. There are two determined parameters, horizontal  $\rho_h$  and vertical  $\rho_v$  resistivity. On the basis of the analysis of phase shift dependence from parameters the following algorithm of the inverse program solution was offered.

Analisis of a form of phase shift isolines allows to present visually problems of a signal interpretation within anisotropic model (Fig. 12). Each isoline sets a set of  $(\rho_h, \rho_v)$  models in which the identical signal is registered. At small angles  $\theta$  resis-



tivity of the isotropic medium, equal  $\rho_h$  can be determined only. At the  $\theta$  values close to  $90^\circ$ , it is possible to make an estimation of  $\rho_h, \rho_v$  variation limit only. Therefore additional criteria of a choice are necessary for unambiguity of the decision. For example, if it is known value  $\rho_h$  (from data in a vertical well), value  $\rho_v$  will be unequivocally determined. At the same time to one value  $\rho_v$  there correspond two values  $\rho_h$  which can strongly differ. The same concerns anisotropy coefficient: to one value  $\Lambda$  also there can correspond two different  $(\rho_h, \rho_v)$  models.

Therefore, the inverse problem is reduced to two following steps. For the set phase shift the set of homogeneous anisotropic models is defined. The concrete model gets out of the found set according to additional criteria. Thus it is considered that the thin pro-layers forming a macroanisotropic layer, are horizontal, that is the angle between a probe and pro-layers is equal to inclinometer data. let's notice that phase shift isolines are almost identical at  $88^\circ < \theta < 92^\circ$ . Therefore practically it is not possible to define little change of  $\theta$  in this range.

The described algorithm is realized in the form of point-to-point processing. As additional criteria of a choice of model on the current point one of the following conditions is used: regularity of horizontal resistivity, regularity of anisotropy coefficient, closeness to the result received on the previous well point, on all considered interval. The last condition means that in the current point of a well there is such model that distance in the  $(\rho_h, \rho_v)$  plane between this model and the model found on the previous point, is minimum. That is, results for the next points of a well are closest of possible.

#### Data inversion

For testing of the program the synthetic signal of a long probe in the anisotropic environment was used:  $\rho_h = 10$ ,  $\rho_v = 70$  ohm·m. Inclinometer data are taken from a horizontal interval of one of wells with horizontal end (length about 170 m). The phase shift was calculated and normally distributed noise was added. The noise range is equal  $\pm 2\%$ . Inversion results and inclinometer data are presented on Fig. 14. It is well visible that the phase shift in the anisotropic medium is almost constant at  $\theta$  limits  $89-91^\circ$ .

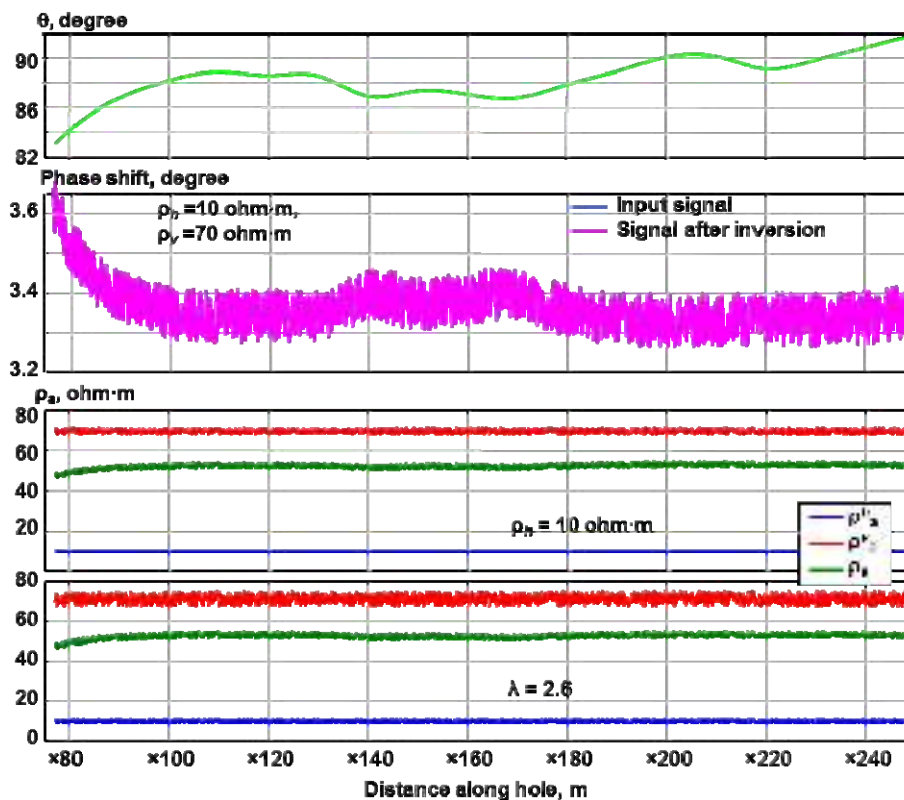


Fig. 14. Angle  $\theta$ , synthetic initial phase shift (with noise) and reconstructed values, reconstructed horizontal and vertical resistivities under condition of fixed  $\rho_h$  and fixed anisotropy coefficient  $\Lambda$ .

Results of point-to-point inversion of a synthetic signal are presented in figure. Value  $\rho_v$  is reconstructed with very high precision at any of three additional conditions if  $\rho_h = 10$  ohm·m in the first point of an interval. Under condition of constancy of  $\rho_h$  the maximum relative deviations of  $\rho_a^v$  are equal  $\pm 2.1\%$ , average value  $\rho_a^v$  equally true. Average  $\rho_a^h$  and  $\rho_a^v$  values are equal 10.3 and 71.4 ohm·m, the maximum relative deviations of  $\rho_a^h$  and  $\rho_a^v$  are equal  $\pm 5.0\%$ , under condition of constancy of anisotropy coefficient.

Let's add of an normally distributed noise with limits of change of  $\pm 1^\circ$  to inclinometer data  $\theta$ . Fluctuations of  $\theta$  are completely transformed to  $\rho_a^v$  changes. Average  $\rho_a^h$  and  $\rho_a^v$  values are equal 10.4 and 71.7 ohm·m at fixed  $\Lambda$ .

Let's note importance of use of apriori information. If the anisotropy coefficient is set incorrectly ( $\Lambda = 2$  at true value 2.65), determined value of  $\rho_a^h$  in 2 times more true value, and value of  $\rho_a^v$  it is more for 16–25 %.

The analysis of practical data revealed major factors which do possible obtaining information on thinly-laminated formations from VEMKZ data. The well way in each interlayer considerably exceeds its thickness when crossing thinly-layered formation at an angle  $70\text{--}90^\circ$ . As a result VEMKZ probes reliably fix alternation of interlayers of the different resistivity which thickness makes from several units to tens centimeters. Influence of mud on responses of the longest probes is insignificant therefore their responses can be interpreted on base of macroanisotropic model. For these probes the amplitude of the fluctuations corresponding to thin lamination, is rather insignificant.

Parameters of electric macroanisotropy are related by known ratios with resistivity and thickness of interlayers of thinly-layered structure. Determination of anisotropy parameters becomes possible if signals are registered on intervals with a different angle between a well and the plane of lamination interlayers borders. Thus this angle can differ from an inclinometer data, as interlayer borders can be not horizontal.

The  $\rho_a^h, \rho_a^v, \theta_a$  values determined as a result of inversion are recalculated in parameters of thin interlayers if there is apriori information. Such information can be the assumption of one interlayer resistivity or about a ratio of thicknesses of different resistivity interlayers. Total thickness of two next interlayers of different resistivity, that is the interlayering period, it is possible to determine using the spectral analysis of signals. After that the estimation of real interlayers thicknesses is carried out. Value of an angle between a probe and the interlayer borders, which is received as a result of inversion, is used for this estimation.

It is possible to estimate fluid type by the offered algorithm in inclined intervals. Let's consider, for example, an interval which length is equal about 200 m (Fig. 15). Mud resistivity is  $\rho_m = 0.05$  ohm·m. Inclinometer data is shown on the bottom. Its size changes in range  $84\text{--}92^\circ$ . Apparent conductivity for the initial and smoothed long probe signals is shown above, and  $\rho_a$  values and  $(\rho_a^h, \rho_a^v, \theta_a)$  model after inversion are shown in the middle of figure.

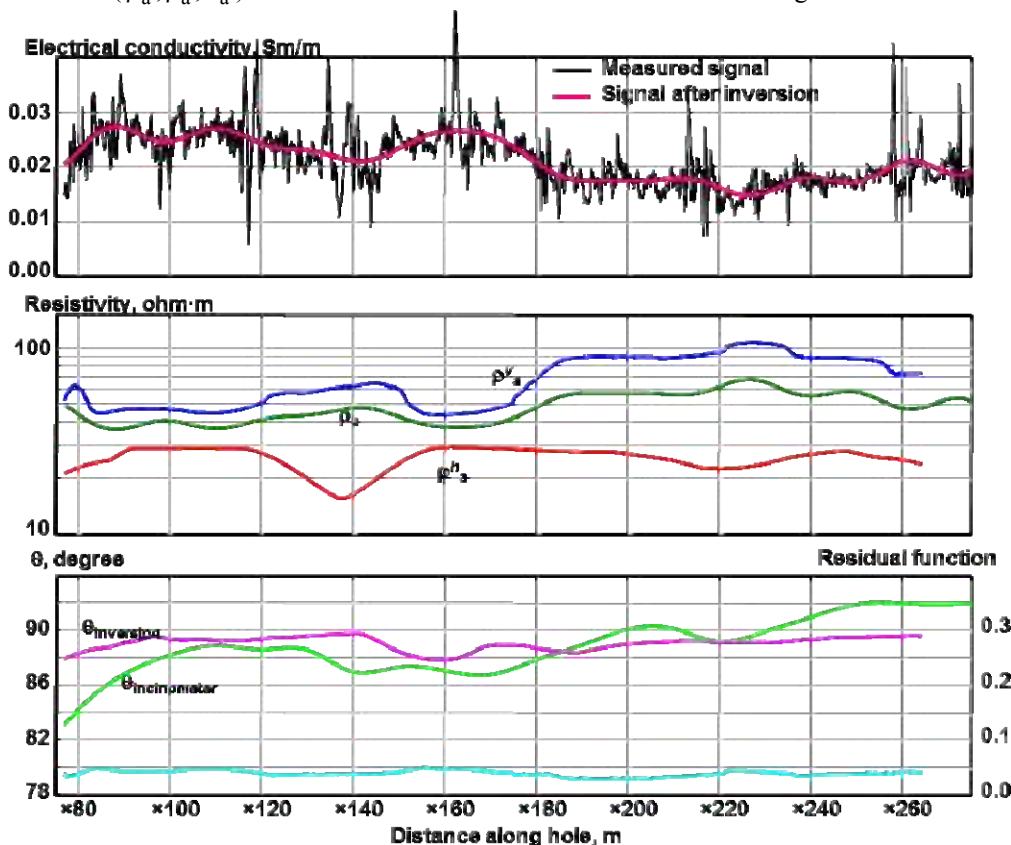


Fig. 15. Measured and smoothed apparent conductivity and after inversion  $\rho_a^h, \rho_a^v, \theta_a$  values. The value closeness to the previous well point result is used as additional criterion.

Quality of the inverse solution is defined by as far as value of residual function is close to zero. Here residual function value don't exceed 0.05 (see Fig. 15). It means that the relative error doesn't exceed 5 %. This value obviously is less than average

dispersion of measured signal equal  $\pm 9\%$ . The error of measurements is equal  $\pm 3\%$ .

The following values of macroanisotropic model parameters are received after inversion of the smoothed long probe signal:  $\rho_a^h = 18\text{--}30\text{ ohm}\cdot\text{m}$ ,  $\rho_a^v = 45\text{--}100\text{ ohm}\cdot\text{m}$ . For average values  $r$  on an interval of 3020–3050 m ( $\rho_a^h = 20\text{ ohm}\cdot\text{m}$ ,  $\rho_a^v = 60\text{ ohm}\cdot\text{m}$ ,  $\theta = 88^\circ$ ) the assessment is made: resistivity of sandy interlayers is about 9 ohm·m, non-permeable interlayers is 80–90 ohm·m. Effective reservoir thickness makes about 40 %, and the thickness of two next interlayers (interlayering period) is equal about 0.15 m.

As in anisotropic model the VEMKZ signal is characterized by some features, it is necessary to choose an interval for inversion proceeding from the following criteria. Algorithms can be used only for processing of the signals measured in subhorizontal intervals ( $\theta = 90 \pm 15^\circ$ ) where high  $\rho_a$  values are observed. For example,  $\rho_a$  in vertical wells is much less, than  $\rho_a$  in a horizontal well. Or there are geological data that on this interval there is the alternation of thin electrically conductive and high-resistivity thin layers that results in resistivity macroanisotropy. Such formation generates high-frequency fluctuations of signals of short probes. The amplitude of these fluctuations usually makes from  $1\text{--}2^\circ$  for wells with fresh mud to  $5\text{--}10^\circ$  for wells with salt high-conductivity mud. In the latter case the high-frequency component also is in signals of averages and long probes. Let's note that one of conditions of successful inversion is that the chosen subhorizontal interval is located rather far from a reservoir top and a bottom.

Thus, possibility of determination of macroanisotropy parameters of thinly-laminated formation from the VEMKZ signals measured in inclined and horizontal intervals is shown. Algorithms of numerical inversion, including on the basis of the analysis of equivalence areas are developed.

### Thin-layered reservoir

Invasion of highly conductive mud into permeable layers of a layered sandy-shales formation leads to increase in resistivity contrast in a invaded zone. VEMKZ signals sensitive to these changes form the oscillating diagrams. This effect becomes more visible in wells with great dip angle (Nikitenko, 2005, Epov, Nikitenko, etc., 2006). In some inclined and horizontal wells the phase shift becomes negative and close to zero. For such values there is no transformation in apparent resistivity calculated both for a homogeneous environment, and taking into account high-conductive well. In subhorizontal intervals VEMKZ signals often look as quasi-periodic functions with small amplitude (Fig. 16, at the left).

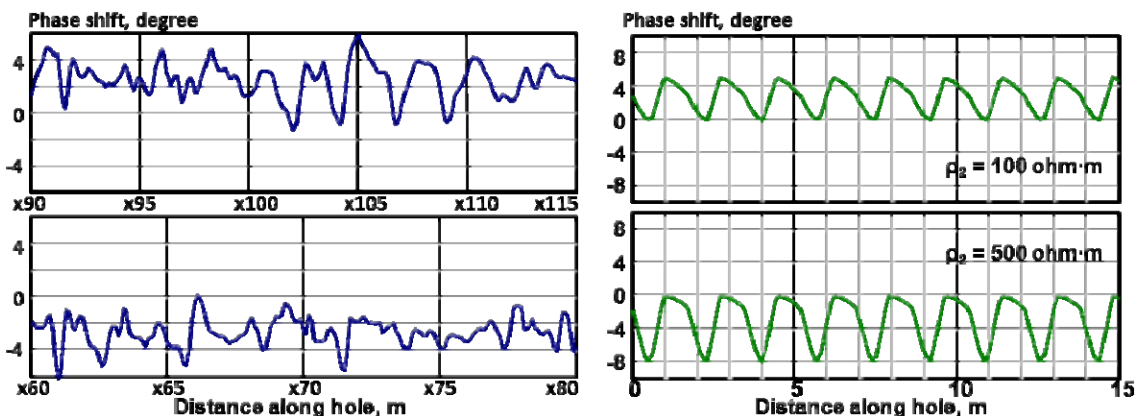


Fig. 16. Signals of a long probe: practical (at the left) and synthetic for models  $\rho_1 = 2.2\text{ ohm}\cdot\text{m}$ ,  $h_1 = 0.2\text{ m}$ ,  $h_2 = 0.1\text{ m}$  (on the right).

Similar type of fluctuation are observed also in the signals measured in a well with a rough wall. The main difference of these situations that roughnesses of a hole wall don't change the average signal level, and thinly-layered high-contrast deposits are usually characterized close to zero and negative average values of a phase shift.

Let's consider the model consisting of high resistive layers and low-resistive layers. Let  $\rho_1, h_1$  and  $\rho_2, h_2$  are resistivities and thickness of pair of alternating layers. Synthetic signals similar to practical signals can be received, when resistivity of conductive layers equally  $1\text{--}2\text{ ohm}\cdot\text{m}$ , and nonconductive –  $100\text{ ohm}\cdot\text{m}$  and above. The total thickness of two next layers is equal 0.3 m, proceeding from Fourier-spectrum of signals. Let's consider that the thickness of conductive clay layers is equal 0.2 m, high-resistive layers thickness is equal 0.1 m (Fig. 16, on the right).

In such model at  $\theta = 80^\circ$  phase shift values fluctuate near zero. For smaller angles or at decrease in electric contrast fluctuations of a signal are displaced in positive area and their amplitudes become less. Decrease of layers thickness and increase in  $\theta$  lead also to decrease in amplitude and to insignificant shift of average value of fluctuations ( $1\text{--}2^\circ$ ). Proportional increase in resistivity of conductive and nonconductive layers also leads to decrease in amplitude. When crossing such packs by a vertical well visible fluctuations of phase shift practically are absent. Signals look as signals in a homogeneous layer with  $\rho_a$  values close to average layer resistivity.

When signal fluctuation closely to periodical, it is possible to estimate  $\rho_1, h_1$  and  $\rho_2, h_2$  values by inversion. As it was

already noted, knowing frequency of fluctuations and  $\theta$ , it is possible to calculate total thickness of the next thin layers. Layers resistivity are determined so that the minimum and maximum values of experimental and synthetic phase shift coincided. The algorithm of inversion realizes a method of nonlinear minimization of a residual function. For decrease in equivalence it is necessary to use apriori information on an formation structure, for example, about possible value of  $\rho_1$  or  $\rho_2$ . The ratio of thickness can be estimated using geometrical characteristics of "positive" and "negative" half waves of signal.

The example of determination of parameters is shown on Fig. 17. The following parameters are determined: a probe tilt angle concerning thin-layer borders –  $80^\circ$ , conductive layers resistivity –  $5.0 \text{ ohm}\cdot\text{m}$  (thickness of  $0.2 \text{ m}$ ), isolating layers resistivity –  $540.0 \text{ ohm}\cdot\text{m}$  (thickness of  $0.1 \text{ m}$ ). The given values describe average model. Parameters of each layer can differ from these values for 10–15 %.

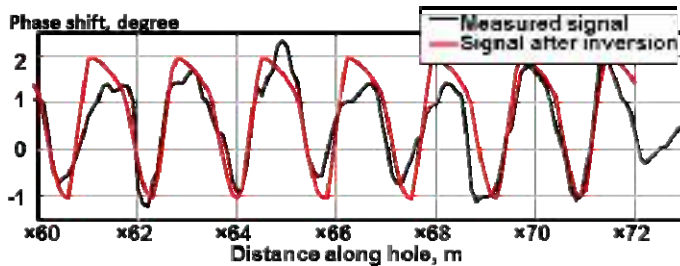


Fig. 17. The measured and synthetic signals of a long probe.

### BKZ in deviated wells

BKZ method has not been used in deviated and horizontal wells; because of the base for electrodes was the logging cable. New logging tool SKL has hard plastic case that allows for recording in the wells of any slope. BKZ signals are generated by direct current and have another dimensional characteristic than induction methods. It can provide additional information about the formation electrical properties. BKZ signals strongly depend on the borehole fluid resistivity and well radius. That's why we can't do the long length probe inversion without the well correction. Now the signals in typical formation models are calculated using numerical modeling. The analysis of obtained results shows that form of BKZ curves helps to establish if crossed high-resistive object is conform to layering thin bed or it is subvertical carbonatized fracture zone.

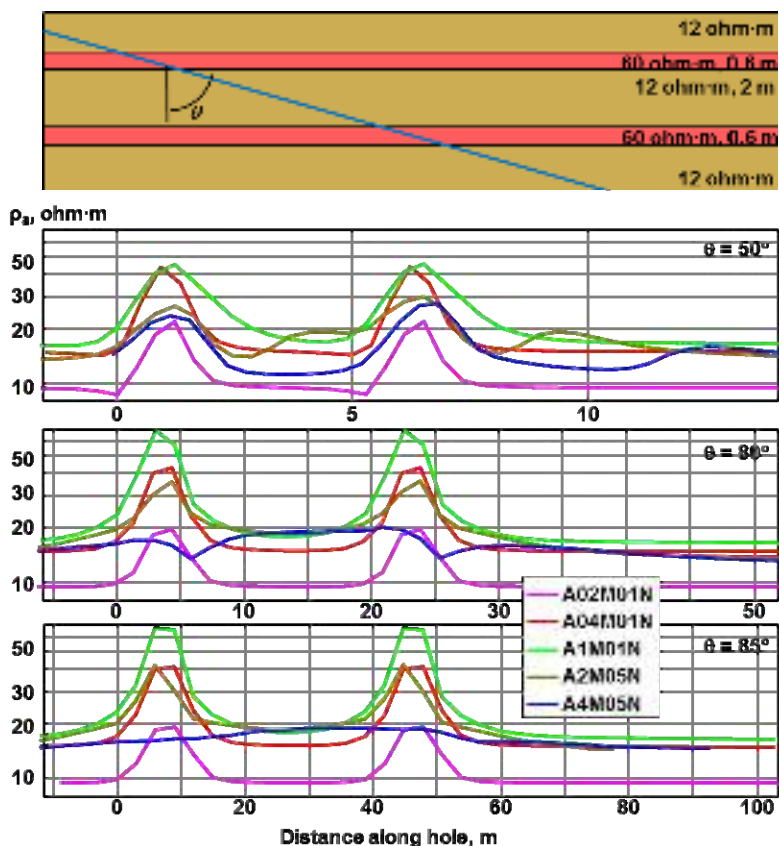


Fig. 18. BKZ signals in deviated well crossing high-resistive layers.

Fig. 18 shows different calculated BKZ curves, BKZ tool intersects low thickness high resistivity formations with different



angles. Well diameter is 0.124 m, tool diameter is 0.102 m, borehole fluid resistivity is 0.3 ohm-m. The curve asymmetry disappears when the angle between tool and formation is low. That's why formation can't be found using 4 meters tool curve. In deviated wells curves have no points of extremum at the formation borders; because of the border intersection is not in the point but in the interval.

Fig. 19 shows the practical BKS data. High values of the neutron logging can be associated with high resistivity objects. For these features of the diagrams can be concluded conformability of high resistivity objects, crossed at intervals of 32-41 and 76-82 m, and the boundaries of objects in the intervals 90-93 and 106-110 m is almost perpendicular to the well. This information is used in the construction of a horizontally layered starting model for inversion of VEMKZ data.

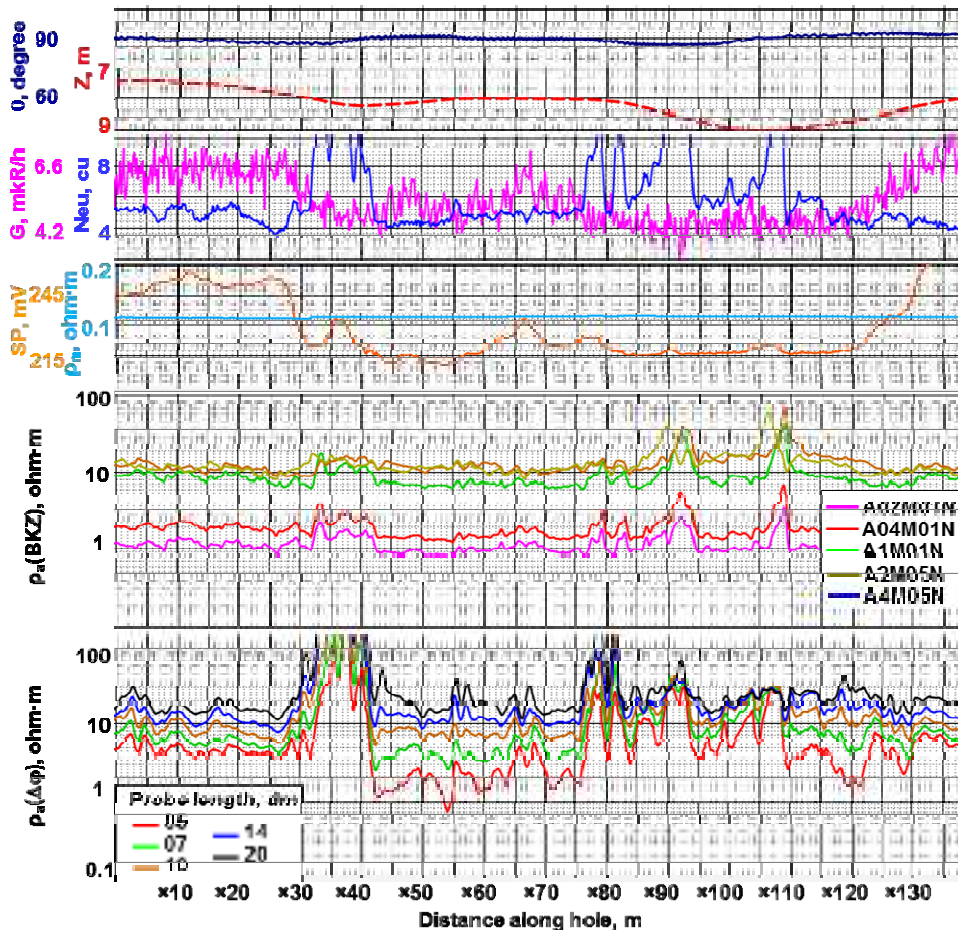


Fig. 19. SKL set data measured in horizontal well.

The first results of numerical simulations show that the BKZ signals depend on the resistivity anisotropy and close electrically contrasting formations differ than VEMKZ signals. Different sensitivity of these methods to geoelectrical model parameters may improve the reliability of the numerical interpretation.

## Conclusions

The created programs of the direct and inverse problem solution allow to interpret VEMKZ signals in typical models of terrigenous collectors at their crossing by inclined and horizontal wells. The starting horizontally layered model is constructed on the basis of the analysis of calculated signal features.

At low mud resistivity influence on VEMKZ signal of small roughnesses of a wall of the well, resulting drilling, leads to emergence of individual or quasiperiodic changes of big amplitude. The average level of a signal is equal to a signal in a smooth well. Influence of eccentricity on long probes signals doesn't exceed an error of measurements. Algorithms of effective numerical correction of influence of wall caves and probe eccentricity are developed.

Based on numerical modeling, possibility of reconstruction of borders location and resistivity of horizontal layers is shown using a VEMKZ signal measured in inclined and horizontal intervals. The approach and algorithms of inversion of a signal of a long probe is offered. One of these algorithms determines of apparent values of horizontal and vertical resistivity and the angle between hole and layer borders. Other algorithm determines resistivities and thicknesses of clay and sandy thin layers in layered formation by the maximum and minimum values and a ratio of width of half waves of a quasi-periodic signal.

## Nomenclature

*BKZ* - Russian lateral logs (direct current non-symmetric tool)  
*VEMKZ* - High-frequency electromagnetic logging sounding  
 $\Delta\varphi$  - phase shift  
 $A_2 / A_1$  - amplitude ratio  
 $\rho_a$  - apparent electrical resistivity  
*SKL* - it is not translated, the name of logging equipment  
 $\rho_h$  - electrical resistivity in horizontal plane  
 $\rho_v$  - electrical resistivity in vertical direction  
 $\theta$  - angle between hole and border plane

## Acknowledgements

We would like to thank Irina Surodina and Oleg Nechaev (IPGG SB RAS), which programs were used for modeling, and 'Surgutneftegaz' company for the practice data.

## References

- Antonov Yu.N., Epov M.I., Kayurov K.N. 2006. VIKIZ in horizontal wells filled by saline biopolymer drilling mud. Karotazhnik, Tver: Gers. No. 9. Pp. 3–21.
- Epov M.I., Kayurov K.N., Yeltsov I.N., Sukhorukova K.V., Petrov A.N., Sobolev A.Yu., Vlasov A.A., 2010. New SKL logging equipment, methods and EMF Pro program for data interpretation. Burenie i nef. Moscow: Burneft. No. 2. Pp. 16–19.
- Epov, M.I., Martakov, S.V., and Suhorukova, K.V. 1999. HILIS diagrams in highly dipping boreholes with penetration zone: Electric and electromagnetic methods of investigation in oil-gas boreholes. Novosibirsk, SB RAS press. Pp. 19–23.
- Epov M.I., Nikitenko M.N., Suhorukova K.V. 2006. About inversion of VIKIZ data measured in thinly-laminated formations in inclined hole. Karotazhnik, Tver: Gers. No.6. Pp.84–100.
- Epov M.I., Shurina E.P., Nechaev O.V., 2007. 3D forward modeling of vector field for induction logging problems. Russian Geology and Geophysics. V. 48, Iss. 9, Pp. 770–774.
- Epov M.I., Suhorukova K.V., Nikitenko M.N. 1999. Resistivity anisotropy evaluation by VIKIZ data. Karotazhnik, Tver: Gers. V.54. Pp.17–29.
- Epov, M.I., Suhorukova, K.V., Nikitenko, M.N., and Antonov, Ju.N. 1998. Application HILIS for logging of horizontal wells: Russian Geology and Geophysics. V. 39. No. 5. Pp. 649–656.
- Epov M.I., Yeltsov I.N., Kashevarov A.A. 2004. Integrated Resistivity and Invasion Model of Invaded Zone. Petrophysics. V. 45. No 2. P. 198.
- Glinskikh V.N. and Epov M.I. 2005. Space sensitivity of relative parameters in high-frequency electromagnetic logging. Russian Geology and Geophysics. No. 11. Pp. 1150–1157.
- Gubina A.I., Giniatov G.Z., Gulanov I.N. 1997. Hole wall trough influence on logging data. Geologiya nefi i gaza. No. 11. Pp.38–42.
- Ignatov V.S., Suhorukova, K.V. Zond eccentricity effects on high-frequency electromagnetic log. 2009. Karotazhnik, Tver: Gers. V. 182. Pp. 101–110.
- Kashevarov A.A., Yeltsov I.N., Epov M.I. 2003. Hydrodynamic model of invaded zone evolution while drilling. Journal of Applied Mechanics and Technical Physics. V. 44, № 6. Pp. 148–157.
- Nikitenko M.N., Shlyk A.V. 2006. New approach to formation electrical resistivity evaluation from VIKIZ data. Karotazhnik, Tver: Gers. No.9. Pp. 3–21.
- Surodina I.V. 2012. Simulation of diagrams BKZ in the boreholes with the highly conductive drilling mud. VIII International Congress "GEO-Sibir", Novosibirsk: SGGA. Proceedings. V.1. Pp. 220–224. <http://geosiberia-2012.ssga.ru/events/conference-2/sekcia-2-2/2-1-Surodina%20I.V.pdf?attredirects=0>
- VIKIZ Method for Logging Oil and Gas Boreholes. Ed. by Epov and Antonov. Novosibirsk: Branch "Geo" of the Publishing House of the SB RAS, 2002, 112 p.
- Zykina M.G., Mamjashev V.G. VIKIZ log features in horizontal well. 2007. Proceedings of International conference for geophysicists and geologists. Tyumen, December 3–7, CD.